Detecting Higgs boson decays to neutralinos at hadron supercolliders

Howard Baer,[1] Mike Bisset,[2] Chung Kao,[1] and Xerxes Tata[2]
[1]*Department of Physics, Florida State University, Tallahassee, Florida 32306*
[2]*Department of Physics and Astronomy, University of Hawaii, Honolulu, Hawaii 96822*
(Received 10 February 1994)

We examine prospects for detecting the neutral Higgs bosons of minimal supersymmetric models (MSSM's) when their decays into neutralino pairs are kinematically allowed. The best signature appears to be $H_h, H_p \to \widetilde{Z}_2\widetilde{Z}_2 \to 4\ell + \not{E}_T$. We argue that standard model contributions to this signature are negligible, and examine regions of MSSM parameter space where the four lepton mode should be observable at the CERN Large Hadron Collider. The same signal can also come from continuum neutralino pair production. We propose a set of cuts to illustrate that the neutralino decay mode of the Higgs bosons provides a viable signal over a substantial range of model parameters, and show that it may be separable from continuum neutralino production if sufficient integrated luminosity can be accumulated.

PACS number(s): 14.80.Cp, 13.85.Qk, 14.80.Ly

I. INTRODUCTION

The derivation of large radiative corrections to Higgs boson masses [1] and couplings in the minimal supersymmetric standard model (MSSM) [2] has led a number of groups [3–7] to reevaluate prospects for supersymmetric (SUSY) Higgs boson detection at various colliding beam facilities. Most of these studies have focused on regions of MSSM parameter space where various standard model (SM) decay modes (e.g., $\gamma\gamma$ and ZZ or $ZZ^* \to 4\ell$) of the SUSY Higgs bosons are detectable above background; parameter space choices were selected such that SUSY particle masses were large so that Higgs boson decays to sparticles were kinematically forbidden. A region of parameter space roughly spanning a Higgs pseudoscalar mass of $m_{H_p} \sim 100 - 300$ GeV and ratio of Higgs vacuum expectation values (VEV's) $\tan\beta \sim 4 - 10$ (for $\tan\beta > 10$, the observability of the signal is sensitive to the detectability of the $\tau\bar{\tau}$ decay modes of the Higgs bosons [9]) was found where *none* of the SM decay modes were detectable [10]. Very recently, it has been argued [11] that Higgs bosons, produced in association with t-quark pairs and identified via their dominant $b\bar{b}$ decays, may fill this "hole," provided that sufficient b-tagging capability can be achieved.

Over the last year or two, several groups [12] have studied grand unified models within the supergravity framework and have shown that it is quite possible to construct models consistent with constraints from colliders, proton decay experiments, and cosmology. Interestingly, these analyses generally find that the sparticles are all considerably lighter than 1 TeV, and further, that the lighter chargino ($\widetilde{W}_1$) and the two lighter neutralinos ($\widetilde{Z}_1$ and $\widetilde{Z}_2$) frequently have masses in the range 50–150 GeV so that these may well be accessible via the decays of the MSSM Higgs bosons.

In Ref. [7], we studied how these supersymmetric decay modes would affect the phenomenology of the Higgs sector. We showed that the chargino and neutralino decays of MSSM Higgs bosons have substantial branching fractions when kinematically allowed, and can sometimes even dominate the usual decay modes. Decays to top squark pairs can similarly be significant since $\tilde{t}_1$, the lighter of the two t squarks, can be much lighter than all other squarks. These new decay channels lead to a diminution of the rate into the standard decay modes so that the above-mentioned hole in parameter space becomes larger. Moreover, the region of parameter space where more than one of the Higgs bosons is visible above background (leading to unambiguous evidence for a nonminimal Higgs sector) is substantially diminished.

One may also ask if the new supersymmetric decay modes of Higgs bosons can lead to new avenues for detection. Decay modes of the neutral Higgs bosons into $\tilde{t}_1\bar{\tilde{t}}_1$ and into $\widetilde{W}_1\widetilde{W}_1$ will lead in general to final states containing $0 - 2$ leptons plus jets plus $\not{E}_T$; at the proposed CERN Large Hadron Collider (LHC) such signals are expected to be buried beneath standard model backgrounds from processes such as top quark pair production. A more promising signature [7] may be found by searching for $H_p, H_h \to \widetilde{Z}_2\widetilde{Z}_2$, where the neutralinos decay leptonically via $\widetilde{Z}_2 \to \ell\bar{\ell}\widetilde{Z}_1$. Such a process leads to a final state with as many as four isolated leptons plus $\not{E}_T$, which is expected to have small SM backgrounds. In addition, kinematic information from the $4\ell + \not{E}_T$ final state can yield information not only on the Higgs boson masses but also on the masses of $\widetilde{Z}_2$ and $\widetilde{Z}_1$ [7]. Signals for invisible decays of Higgs bosons via $H_\ell \to \widetilde{Z}_1\widetilde{Z}_1$ have also been considered [8].

In this paper, we seek to expand upon and improve the calculations presented in Ref. [7] regarding signals from supersymmetric decays of the Higgs bosons. In particular, we incorporate radiative corrections to the SUSY Higgs boson masses and couplings, from both top and bottom Yukawa interactions, and effects from mixing be-

tween third generation squarks, we include Higgs boson decays into squarks and sleptons—these can be very important since decays to $\tilde{t}_1$ pairs may be allowed, we have included Higgs boson production via $b\bar{b}$ fusion, which is the main production mechanism for large values of $\tan\beta$, and we have included effects from nondegenerate squark and slepton masses, which can lead to enhanced [13] leptonic decays of the neutralino, resulting in a much larger signal.

The rest of this paper is organized as follows. In Sec. II, we describe in some detail the improvements and extensions we have made to our earlier calculation. In Sec. III, we present cross sections for the various signals as a function of model parameters. In Sec. IV, we present background calculations, and suggest a set of experimental cuts useful for extracting the signal. We also estimate efficiencies due to these cuts. In Sec. V, we present our conclusions regarding detectability of the SUSY Higgs bosons via both the standard model decays as well as via the supersymmetric 4ℓ signal, along with a summary of our results.

II. CALCULATIONAL DETAILS

As in Ref. [7], we have computed the masses and mixing angles in the Higgs boson sector using the one-loop effective potential. We have, however, improved on our previous calculation in several respects. We now include the effects of both top and bottom family Yukawa interactions (the latter interactions, which were neglected in Ref. [7], can be important if $\tan\beta$ is large) as well as effects from supersymmetric and SUSY-breaking trilinear scalar interactions of the scalar top (scalar bottom) Higgs system. These trilinear couplings lead to mixing between the L- and R-type sfermions, and so further reduce the mass of the lighter mass eigenstate. This can be especially important for t squarks, whose mass is already expected to be smaller than that of other squarks on account of the large top Yukawa coupling, since the branching fraction for the $\tilde{t}_1\bar{\tilde{t}}_1$ decay mode can be very large if $m_{\tilde{t}_1} < m_t$. Finally, we have also included D-term contributions [14] to the effective potential, but generally speaking, their effects are small.

These modifications lead to improvements in the calculation of some of the decay modes of the Higgs bosons. First, radiative corrections at the same level as those mentioned in the last paragraph are incorporated into the calculation of the H_h-H_ℓ-H_ℓ vertex. Second, Higgs boson decays into sfermions are now added. As mentioned, the sfermion masses including D terms have been calculated with intraflavor mixing from nonzero values for A_t, A_b, and μ. These modifications to squark masses and mixings also affect the loop decays of the Higgs bosons into two gluons which, in turn, affects Higgs boson production by gluon fusion.

In the MSSM, the bottom quark Yukawa coupling is inversely proportional to the parameter $\cos\beta$. Hence, the $H \to b\bar{b}$ width (here, H is a generic Higgs boson) as well as the subprocess cross section $\hat{\sigma}(b\bar{b} \to H)$ are enhanced in regions of large $\tan\beta$. In our calculations, we include Higgs boson production cross sections via gg and $b\bar{b}$ fusion. The formula for $\hat{\sigma}(gg \to H)$ is well known [15]; for $b\bar{b}$ fusion, we use the result

$$\sigma(pp \to b\bar{b} \to HX) = \frac{16\pi^2}{m_H^3}\frac{1}{4}\frac{1}{9}\frac{\Gamma(H \to b\bar{b})}{\lambda^{\frac{1}{2}}(1, m_b^2/m_H^2, m_b^2/m_H^2)}\tau \times F_{\rm DW} \tag{2.1}$$

$$\times \int_\tau^1 \frac{dx}{x}[D_{b/p}(x,Q^2)D_{\bar{b}/p}(x/\tau,Q^2) + (b \leftrightarrow \bar{b})] \tag{2.2}$$

where $\tau = m_H^2/s$, $D_{b/p}(x,Q^2)$ is the b parton distribution function in the proton, and

$$F_{\rm DW} = [16.2 - 4.28\ln(m_H) + 0.31(\ln(m_H))^2]^{-1} \tag{2.3}$$

(with m_H in GeV) is a fit to the results of Ref. [16] to incorporate contributions of higher-order graphs to the $b\bar{b}$ fusion mechanism. We use the Eichten-Hinchliffe-Lane-Quigg (EHLQ) set 1 [17] b and g parton distributions, and take the SM parameters to be $m_b = 5$ GeV, $\sin^2\theta_W = 0.23$, $\alpha_s(M_Z{}^2) = 0.118$ with $\Lambda_4(\text{QCD}) = 0.177$.

It has been pointed out in Ref. [13] that leptonic decays of neutralinos can be enhanced by large factors if squarks are significantly heavier than sleptons (as is the case in the "no-scale" [18] limit), and the $Z\widetilde{Z}_1\widetilde{Z}_2$ coupling is dynamically suppressed. This suppression is common in supergravity models with radiative electroweak symmetry breaking since, in this case, $|\mu| \simeq m_{\tilde{g}}$ [2,12]—as a result, $\widetilde{Z}_1$ and $\widetilde{Z}_2$ are, respectively, mainly U(1) and SU(2) gauginos and so have suppressed couplings to the Z boson. We calculate slepton masses as usual by using renormalization group equations to evolve sfermion masses from a common grand unified theory (GUT) scale scalar mass to their weak scale values [19]. In our computation of the neutralino mass matrix we have, as usual, assumed that the modified minimal subtraction scheme ($\overline{\rm MS}$) gaugino masses unify at some ultrahigh energy scale. We then evolve these down to the electroweak scale. However, in the following, we present our results in terms of the physical pole gluino mass which we relate to the corresponding $\overline{\rm MS}$ mass using the result of Ref. [20]. Finally, we note that we have not included QCD corrections to Higgs production and decay via loops [21].

III. THE 4-LEPTON SIGNAL FROM NEUTRALINO DECAYS OF HIGGS BOSONS

Once the various Higgs boson production cross sections via gg and $b\bar{b}$ fusion as well as the $H \to \widetilde{Z}_2\widetilde{Z}_2$ and $\widetilde{Z}_2 \to \ell\bar{\ell}\widetilde{Z}_1$ branching ratios are known, the total rate for $\sigma(pp \to H \to \widetilde{Z}_2\widetilde{Z}_2 \to 4\ell + 2\widetilde{Z}_1)$ can be calculated. The cross section is a function of the MSSM model parameters $(m_{\tilde{g}}, m_{\tilde{q}}, m_{\tilde{t}_L}, m_{\tilde{t}_R}, m_{\tilde{b}_L}, \mu, \tan\beta, m_{H_p}, A_t, A_b, m_t)$; the slepton masses are related as given in Ref. [13]. Of course, in supergravity models with radiative electroweak symmetry breaking, there is some correlation amongst

these parameters: typically, μ scales with $m_{\tilde{g}}$, and m_{H_p} is strongly correlated with μ and the universal GUT scale scalar mass. The parameter choices used in this paper to illustrate our results are inspired, but not ruled, by the supergravity mass relations.

We begin by showing in Fig. 1 a contour plot in the m_{H_p} vs $\tan\beta$ plane of $\sigma(pp \to H \to \widetilde{Z}_2\widetilde{Z}_2 \to 4\ell + \not{E}_T)$ ($\ell = e$ or μ) in fb, at $\sqrt{s} = 14$ TeV. We take $m_{\tilde{g}} = -\mu = m_{\tilde{q}} = 300$ GeV, while $A_t = A_b = 0$, and $m_t = 165$ GeV. The scalar top masses are set at their default values: $m^2_{\tilde{t}_L} = m^2_{\tilde{q}} - 50$ GeV^2, and $m^2_{\tilde{t}_R} = m^2_{\tilde{q}} - 100$ GeV^2. The region in black is excluded by the nonobservation of supersymmetry signals in experiments at the CERN e^+e^- collider (LEP) as parametrized in Ref. [7] but taking into account the recent limit of 63.5 GeV on the mass of the SM Higgs boson [22]. Fig. 1(a) shows results for $H = H_p$, while Fig. 1(b) shows results for $H = H_h$. We note the following features.

The $H_p \to 4\ell$ cross section exceeds 500 fb for small values of $\tan\beta$ and $m_{H_p} \sim 300$ GeV, just below threshold for $H_p \to t\bar{t}$ decay whereas the corresponding cross section from H_h does not exceed 100 fb. Over a wide range of parameters, away from $\tan\beta = 1$, the two processes

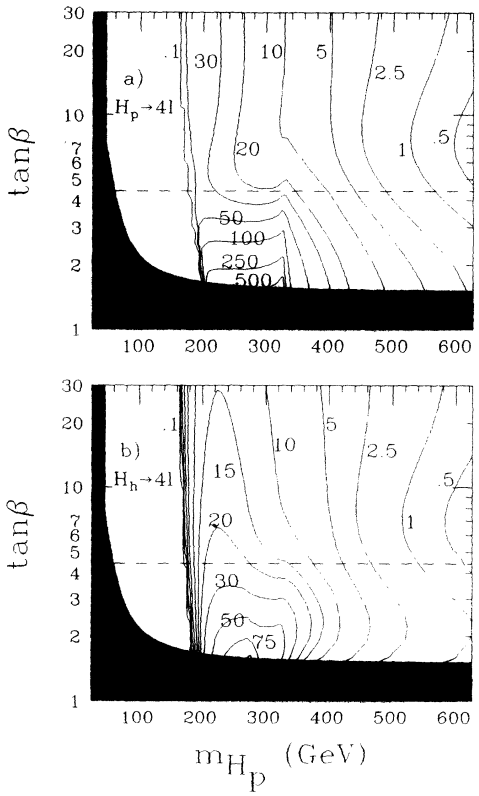

FIG. 1. Contour plot of cross section in fb for (a) $pp \to H_p \to \widetilde{Z}_2\widetilde{Z}_2 \to 4\ell + \not{E}_T$ and (b) $pp \to H_h \to \widetilde{Z}_2\widetilde{Z}_2 \to 4\ell + \not{E}_T$ events, in the m_{H_p} vs $\tan\beta$ plane, at $\sqrt{s} = 14$ TeV. We take $m_{\tilde{q}} = m_{\tilde{g}} = -\mu = 300$ GeV, $m_t = 165$ GeV, and $A_t = A_b = 0$. We also take $m^2_{\tilde{t}_L} = m^2_{\tilde{q}} - 50$ GeV^2 and $m^2_{\tilde{t}_R} = m^2_{\tilde{q}} - 100$ GeV^2. The region above the dashed lines corresponds to $m_{\widetilde{W}_1} < 90$ GeV, the approximate reach of LEP II. The reach of LEP II for detection of Higgs boson signals is shown in Fig. 7(b).

give comparable cross sections. The large difference between the scalar and pseudoscalar contributions to the signal for small values of $\tan\beta$ mainly comes from the difference in their SUSY branching fractions [7].

The signal from the decays of H_p and H_h are separately larger than 5 fb for 200 GeV $< m_{H_p} <$ 400 GeV. Since H_h and H_p are expected to be roughly degenerate over the range of masses where the signal is significant, this corresponds to a total of 250–25 000 4ℓ events at the LHC before any selection cuts, assuming a data sample with 50 fb^{-1}. Interestingly, the signal has a larger rate in the region below the dashed line, where the lighter chargino is heavier than 90 GeV, which we take to roughly represent the supersymmetry reach of LEP II (We note that this region is rather sensitive to the precise value of the chargino mass reach that is assumed). The Higgs bosons H_ℓ and H_p may themselves be directly accessible at LEP II. The range of parameters where this is possible is discussed in the last section and illustrated in Fig. 7 for one choice of parameters.

Although we have not shown this, we have checked that for values of $\tan\beta \lesssim 4$, both H_h and H_p cross sections are dominated by gluon fusion, while $b\bar{b}$ fusion, which was ignored in Ref. [7], dominates for $\tan\beta \gtrsim 10$.

The cross section for $4\ell + \not{E}_T$ events has an observable rate in part of the "hole region," where $3 < \tan\beta < 10$–20 and $100 \lesssim m_{H_p} \lesssim 200$–$300$ GeV. This is the region where no SM decays of MSSM Higgs boson are observable (except for possible observation of $H \to b\bar{b}$). Of course, the range over which this signal might be observable is sensitive to μ and $m_{\tilde{g}}$ since the cross section drops sharply to zero when the kinematic limit for the decays $H_{p,h} \to \widetilde{Z}_2\widetilde{Z}_2$ is approached.

The contours of the 4ℓ cross section are shown in the $\mu - \tan\beta$ plane in Fig. 2 for (a) H_p decays and (b) H_h decays. The pseudoscalar mass is fixed to be 250 GeV, which is within the hole region for the light $\widetilde{W}_1$ and $\widetilde{Z}_{1,2}$ case illustrated here. Other parameters are as in Fig. 1. We see that the signal cross section exceeds 10 fb for a wide region of parameter space. Again, the black region is excluded by LEP constraints, and the dashed line is the contour $m_{\widetilde{W}_1} = 90$ GeV (the region above the dashed contour has $m_{\widetilde{W}_1} < 90$ GeV). In the upper corners of Fig. 2, $m_{\tilde{\tau}} < 45$ GeV, because of τ Yukawa interactions which have substantial effects for large values of $\tan\beta$ [23]. While the signal is small for small values of $|\mu|$, it is instructive to see that the 4ℓ rate appears to be observable for $|\mu| \simeq m_{\tilde{g}}$ as expected in supergravity models with radiative electroweak (EW) symmetry breaking. Finally, we observe that the pseudoscalar Higgs boson tends to give a larger signal than the heavy scalar, and further, that the signal is significantly larger if μ happens to be negative in our convention.

In Fig. 3, we study the dependence of the signal on the squark mass for a fixed value of $m_{\tilde{g}}$. Here, m_{H_p} is fixed at 250 GeV; other parameters are as in Fig. 1. We see that the 4ℓ cross section rapidly drops off as $m_{\tilde{q}}$ increases from $m_{\tilde{g}}$ to larger values. For values of $\tan\beta \gtrsim 5$, the cross section shows a slow increase for rather large squark masses. As expected, the squark mass dependence of the

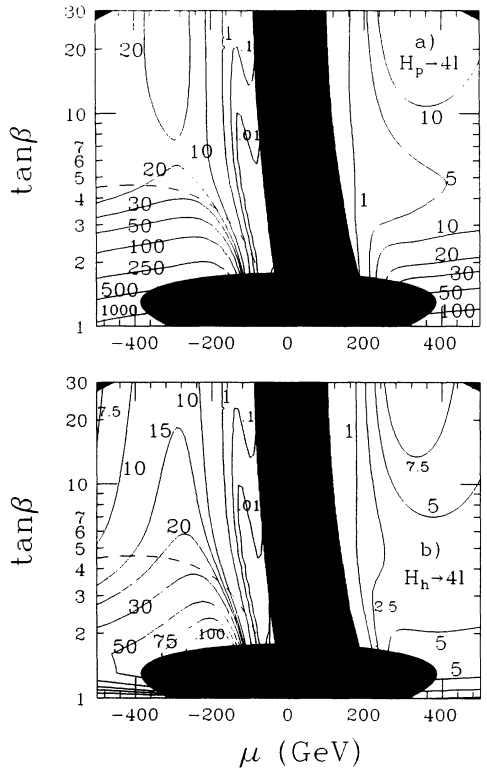

FIG. 2. Contour plot of cross section in fb for (a) $pp \to H_p \to \widetilde{Z}_2\widetilde{Z}_2 \to 4\ell + \not{E}_T$ and (b) $pp \to H_h \to \widetilde{Z}_2\widetilde{Z}_2 \to 4\ell + \not{E}_T$ events, in the μ vs $\tan\beta$ plane, at $\sqrt{s} = 14$ TeV. Parameters are as in Fig. 1, except $m_{H_p} = 250$ GeV. The region above the dashed contour corresponds to $m_{\widetilde{W}_1} < 90$ GeV.

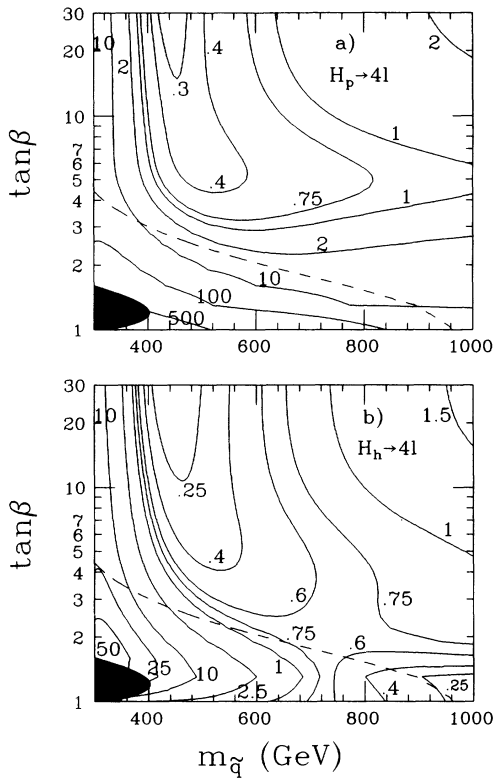

FIG. 3. Contour plot of cross section in fb for (a) $pp \to H_p \to \widetilde{Z}_2\widetilde{Z}_2 \to 4\ell + \not{E}_T$ and (b) $pp \to H_h \to \widetilde{Z}_2\widetilde{Z}_2 \to 4\ell + \not{E}_T$ events, in the $m_{\tilde{q}}$ vs $\tan\beta$ plane, at $\sqrt{s} = 14$ TeV. Parameters are as in Fig. 1, except $m_{H_p} = 250$ GeV. The region above the dashed contour corresponds to $m_{\widetilde{W}_1} < 90$ GeV.

cross section is mostly determined by that of the leptonic branching fraction of the $\widetilde{Z}_2$. For $m_{\tilde{q}} \simeq m_{\tilde{g}}$, the sleptons are considerably lighter than the squarks resulting [13] in an enhancement of $\widetilde{Z}_2 \to \ell\bar{\ell}\widetilde{Z}_1$ decays, and hence, in the 4ℓ cross section. The increase in the cross section for large values of $m_{\tilde{q}}$ comes from interference between various amplitudes. We see that the signal has an observable rate even if squarks are significantly heavier than gluinos. Amusingly, the cross section is largest below the dashed line where the chargino is likely to be undetectable at LEP II.

Before closing this discussion we mention that we have checked that the 4ℓ cross section is relatively insensitive to the A parameters or to the precise value of m_t except when the threshold for a new decay is crossed. This is especially important when considering the variation of the signal with A_t, since $H \to \tilde{t}_1\bar{\tilde{t}}_1$ decays become kinematically accessible when $|A_t|$ becomes very large. Finally, we have also studied the variation of the signal with $m_{\tilde{g}}$. For $m_{H_p} = 250$ GeV, and $-\mu = m_{\tilde{q}} = m_{\tilde{g}}$, the signal exceeds 5 fb for gluinos as heavy as 350–400 GeV. This is reasonable since then, $m_{\widetilde{Z}_2} \simeq= m_{\tilde{g}}/3$ is approaching the kinematic boundary of $H_p \to \widetilde{Z}_2\widetilde{Z}_2$ decays.

IV. BACKGROUNDS, CUTS, AND EFFICIENCIES

We have seen that the neutralino decays of the pseudoscalar and the heavy neutral scalar Higgs bosons of the MSSM can result in several hundred to several thousand events with four isolated leptons together in an LHC data sample of 50 fb^{-1}. These events should be very distinctive since, except for QCD radiation, they would be free of hadronic activity. Within the SM, isolated leptons mainly arise from the production and decays of the W and Z bosons and of the top quark. The main background from ZZ pair production can be efficiently removed by vetoing events where like-flavor, opposite sign leptons reconstruct the Z mass within ± 10 GeV. We have verified this by generating 10 000 ZZ events using ISAJET (and forcing the leptonic decay of the Z bosons). No events are found after the mass cut, resulting in an upper bound on the 4ℓ cross section of about 0.003 fb. This would, of course, also remove the signal if the decay $\widetilde{Z}_2 \to \widetilde{Z}_1 Z$ is kinematically accessible; fortunately for the range of parameters where we find the signal to be substantial, this decay is kinematically inaccessible,

so that this requirement results in very little loss of the signal. The signal can also be mimicked by $\bar{t}tZ$ or $4t$ production. These backgrounds can easily be removed by vetoing events with a central jet in addition to the Z mass veto already mentioned. The main SM physics background thus comes from electroweak multi-W production. At the LHC, the trilepton cross section from $3W$ production has been shown [24] to be about 2 fb, so that the background to the signal from $4W$ production should be negligible. Because the cross section for $t\bar{t}$ production at the LHC is very large, one may also worry that these may provide a significant background when the leptons from the daughter bottom quarks are accidently isolated; a simulation of 300 000 $t\bar{t}$ events with forced top quark decays yielded no background, giving a limit $\sigma(t\bar{t}) < 4$ fb. We have been unable to identify any significant SM sources of physics backgrounds to the SUSY Higgs boson signal.

Within the MSSM framework, however, the continuum production of $\widetilde{Z}_2$ pairs [25] can also result in the same signal. These are produced by $q\bar{q}$ annihilation via s-channel Z exchange or t- and u-channel squark exchange. While the detection of these continuum neutralino pairs would in itself be very exciting, it is interesting to ask whether $\widetilde{Z}_2\widetilde{Z}_2$ production via H_h and H_p decays is distinguishable from the continuum production of $\widetilde{Z}_2$ which, in effect, is the background to our Higgs signal. Toward this end, we have shown in Fig. 4 the cross section for 4ℓ production via continuum $\widetilde{Z}_2\widetilde{Z}_2$ production as a function of $\tan\beta$. To compare with $\widetilde{Z}_2$ production via Higgs boson decays discussed in the last section, we have taken $m_{\tilde{g}} = \pm\mu = 300$ GeV and illustrated our results for $m_{\tilde{q}} = m_{\tilde{g}}$ (solid line) and $m_{\tilde{q}} = 2m_{\tilde{g}}$ (dashed line). The pseudoscalar Higgs boson mass is fixed to be 250 GeV and other parameters are fixed as in Figs. 1–3. We see that while the cross section is sensitive to the squark mass it is relatively insensitive to $\tan\beta$ over the region where the cross section is significant. Furthermore, for $m_{\tilde{g}} = m_{\tilde{q}}$, the cross section is 10–30 fb which is generally comparable to, or smaller than, the cross sections in Fig. 2 for a wide range of parameters.

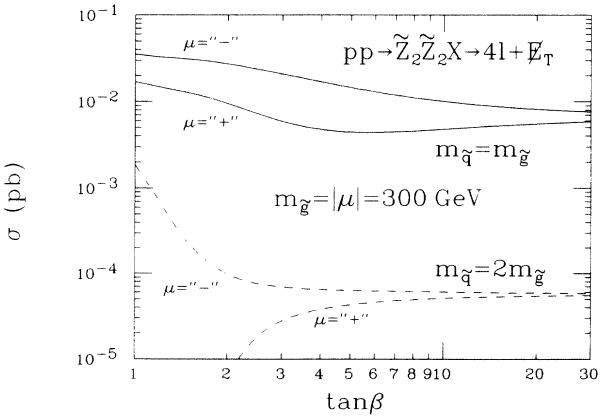

FIG. 4. Cross section in pb for continuum $pp \to \widetilde{Z}_2\widetilde{Z}_2 \to 4\ell + \not{E}_T$ production vs $\tan\beta$ for $m_{\tilde{g}} = \pm\mu = 300$ GeV, at $\sqrt{s} = 14$ TeV.

We use ISAJET 7.07 [26] to simulate the 4ℓ Higgs boson signal. Since explicit SUSY Higgs production has not yet been incorporated into this code, we simulate the production of H_h or H_p by decaying the SM Higgs scalar into a $\widetilde{Z}_2$ pair and forcing the SUSY decay mode; the total cross section is then normalized to the results of Figs. 1–3.

We use the toy calorimeter simulation package ISAPLT to model detector effects. We simulate calorimetry with cell size $\Delta\eta \times \Delta\phi = 0.1 \times 0.1$, which extends between $-5 < \eta < 5$ in pseudorapidity. We take electromagnetic energy resolution to be $10\%/\sqrt{E_T} \oplus 0.01$, while hadronic resolution is $50\%/\sqrt{E_T} \oplus 0.03$ for $|\eta| < 3$, and $100\%/\sqrt{E_T} \oplus 0.07$ for $3 < |\eta| < 5$, where $\oplus$ denotes addition in quadrature. Jets are coalesced within cones of $R = \sqrt{\Delta\eta^2 + \Delta\phi^2} = 0.7$ using the ISAJET routine GETJET. Hadronic clusters with $E_T > 50$ GeV are labelled as jets. Muons and electrons are classified as isolated if they have $p_T > 10$ GeV, $|\eta(\ell)| < 2.5$, and the visible activity within a cone of $R = 0.3$ about the lepton direction is less than $E_T(\text{cone}) = 2$ GeV.

We then impose the following cuts designed to select signal events, while vetoing SM backgrounds from ZZ and $t\bar{t}$ production: require *two* isolated leptons with $p_T(\ell) > 20$ GeV to trigger the event; require *two* more isolated leptons with $p_T(\ell) > 10$ GeV; require all opposite sign but same flavor dilepton pairs to have invariant mass $m(\ell\bar{\ell}) < 80$ GeV or $m(\ell\bar{\ell}) > 100$ GeV; require number of jets $n(\text{jets}) = 0$. A cut on $\not{E}_T$ could be considered instead of the above dilepton mass cut. However, the $\not{E}_T$ spectrum from the signal is not so hard, while forward jet production and energy mismeasurement in ZZ events can lead to substantial $\not{E}_T$, so that the dilepton mass cut wins over an $\not{E}_T$ cut in rejecting background while preserving signal.

We should stress that there are no significant SM backgrounds even before the last cut. Backgrounds involving the Z are efficiently removed by the $m(\ell\bar{\ell})$ cut. The main physics background would then be expected to come from $4t$ production which gives a 4ℓ cross section around 0.05 fb at the LHC, even before acceptance cuts [27]. The last cut which removes about 40% (70%) of the signal for a Higgs boson mass around 200 GeV (400 GeV) has been imposed to separate neutralino production from the cascade decays of gluinos and squarks [28] which can also produce multilepton events at observable rates.

In order to give the reader an idea of the impact of the cuts on the 4ℓ signal, we have shown these cross sections for illustrative choices of m_{H_p} and $\tan\beta$ in Table I. We have added the contributions from H_h and H_p decays since these are expected to lead to kinematically similar events. We have also shown the continuum background for the same choices of parameters. The following points are worth noting.

For the choice of parameters in the table, the signal exceeds the background for m_{H_p} up to somewhat beyond 300 GeV, where $t\bar{t}$ decays become accessible. Also, the cross section corresponds to an event rate 100–1000 events after cuts in a 50 fb^{-1} data sample, compared to

TABLE I. Cross sections in fb at LHC for $4\ell + \not{E}_T$ events from supersymmetric processes. We take $m_{\tilde{g}} = 300$ GeV and $\mu = -m_{\tilde{g}}$, while $m_{\tilde{q}} \sim m_{\tilde{g}}$ and $A_t = 0$.

Process	m_{H_p}	$\tan\beta$	$m_{\widetilde{Z}_2}$	$m_{\widetilde{Z}_1}$	$\sigma(4\ell)$	σ(cut)	Effic.	χ^2
$H_h, H_p \to 4\ell$	200	2	97.3	45.5	230	26	11%	18036
$H_h, H_p \to 4\ell$	300	2	"	"	260	23	9%	1024
$H_h, H_p \to 4\ell$	400	2	"	"	37	2.4	6.5%	23
$\widetilde{Z}_2\widetilde{Z}_2 \to 4\ell$	–	2	"	"	27	2.8	10%	–
$H_h, H_p \to 4\ell$	200	10	83.4	42.8	44	2.4	5.5%	528
$H_h, H_p \to 4\ell$	300	10	"	"	26	1.4	5.4%	32
$H_h, H_p \to 4\ell$	400	10	"	"	10	0.5	5%	4.5
$\widetilde{Z}_2\widetilde{Z}_2 \to 4\ell$	–	10	"	"	10	0.8	8%	–

a continuum background of 50–100 events.

The signal efficiency varies between 5 and 10 percent depending on the model parameters; Figs. 1–3 can thus be used to estimate the signal after the cuts.

It should, of course, be kept in mind that the SUSY parameters are not known, and that the total background (and signal) rate could be considerably different (even for similar values of $m_{\widetilde{Z}_2}$) from our estimate in the table.

An excess of the 4ℓ events relative to the background in Table I would, therefore, not enable us to infer cleanly a Higgs boson signal. Instead, we consider the possibility of separating the signal from the continuum background by studying the invariant mass distribution of the four leptons: for the signal, we must have $m(4\ell) < m_H - 2m_{\widetilde{Z}_1}$, while the background should exhibit a rather broad distribution. Since these distributions are determined by the Higgs boson and neutralino masses, we expect them to be relatively insensitive to variations in model parameters which result in similar values of m_H, $m_{\widetilde{Z}_1}$, and $m_{\widetilde{Z}_2}$.

Toward this end, we have shown in Fig. 5 and Fig. 6 these distributions for the signal plus background (solid) and the $\widetilde{Z}_2\widetilde{Z}_2$ continuum "background" (dashed) for the six cases in Table I. For the smaller values of m_{H_p}, the solid histograms are dominated by the signal and differ considerably from the dashed background histograms (note that these are shown using a log scale). As anticipated above, the solid and dashed lines indeed coincide for $m(4\ell) > m_{H_p} - 2m_{\widetilde{Z}_2}$. In order to decide whether the solid and dashed histograms are indeed distinguishable, we have computed the total χ^2 for the difference between these two histograms, *normalized to the same number of*

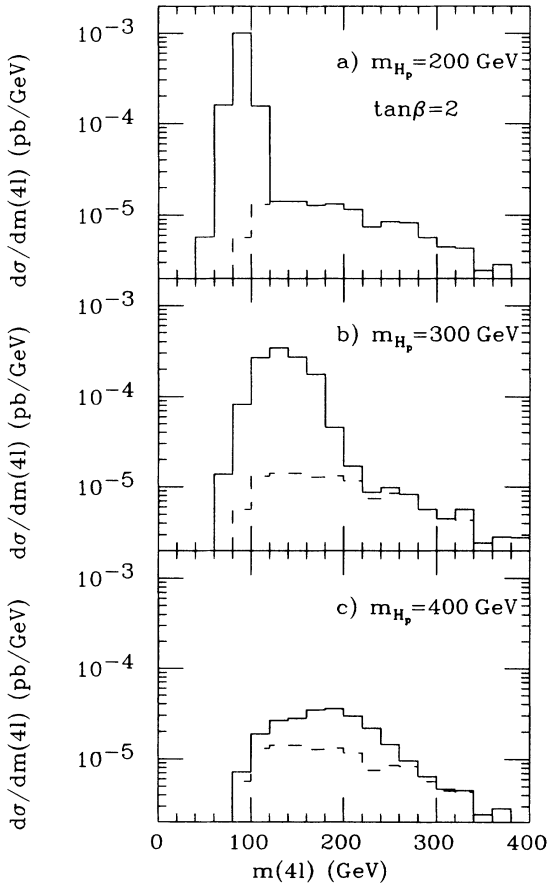

FIG. 5. Distribution in $m(4\ell)$ after cuts from signal plus background (solid), and background (dashes) for $pp \to H_p, H_h \to \widetilde{Z}_2\widetilde{Z}_2 \to 4\ell + \not{E}_T$ production for $\tan\beta = 2$ for (a) $m_{H_p} = 200$ GeV, (b) $m_{H_p} = 300$ GeV, and (c) $m_{H_p} = 400$ GeV. Other parameters are as in Fig. 1.

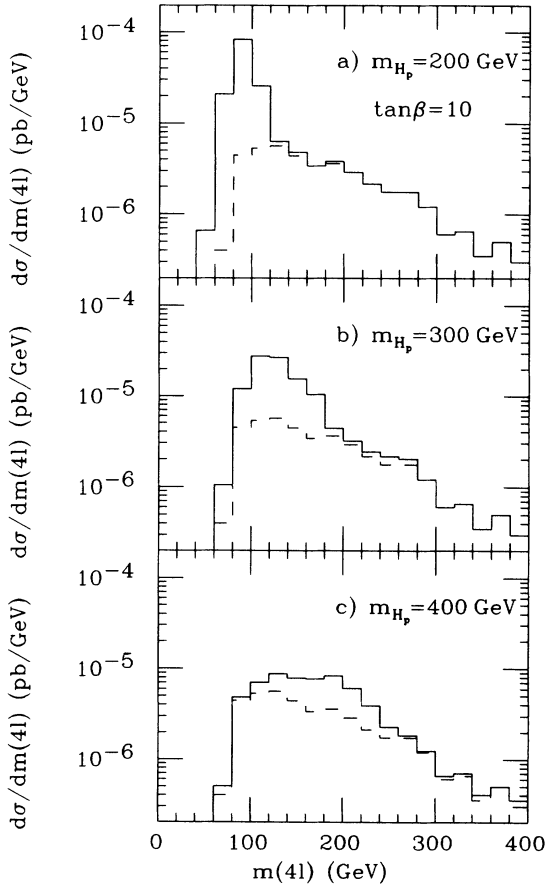

FIG. 6. Distribution in $m(4\ell)$ after cuts from signal plus background (solid), and background (dashes) after cuts for $pp \to H_p, H_h \to \widetilde{Z}_2\widetilde{Z}_2 \to 4\ell + \not{E}_T$ production for $\tan\beta = 10$ for (a) $m_{H_p} = 200$ GeV, (b) $m_{H_p} = 300$ GeV, and (c) $m_{H_p} = 400$ GeV. Other parameters are as in Fig. 1.

events, with the event number given by the signal plus background cross section times an integrated luminosity of 50 pb^{-1}. In this computation, we have used twelve 20 GeV bins between $m(4\ell) = 60$ GeV and $m(4\ell) = 300$ GeV. In our simulation, we have about 1100, 900, and 600 events for $m_{H_p} = 200$, 300, and 400 GeV (after cuts) for the $\tan\beta = 2$ case, and about 550 events for each value of m_{H_p} for $\tan\beta = 10$. The resulting total χ^2 is shown in the last column of Table I. It thus appears that for $m_{H_p} \lesssim 300$ GeV, the distributions are sufficiently different that the solid line is unlikely to be a chance fluctuation of the continuum background (for $\chi^2 > 26.2$, this probability is smaller than 1%). Some remarks are, however, in order.

Despite the fact that we have normalized the solid and histograms to have the same number of events, our conclusion clearly depends on the relative number of Higgs bosons initiated and continuum $\widetilde{Z}_2\widetilde{Z}_2$ events. Here, we have used the rate as given by the MSSM for the values of parameters motivated by supergravity models.

For the first two cases in Table I, the number of events in our simulation is comparable to the expected number in a data sample of 50 fb^{-1}. We thus expect our computation of the total χ^2 to be a reasonable reflection of the experimental situation. For the $\tan\beta$=10 case, with $m_{H_p} = 200$ GeV (300 GeV), the signal cross section is much smaller so that about 200 fb^{-1} (400 fb^{-1}) of integrated luminosity need to be collected in order that the fluctuations in our simulation are of comparable magnitude to those in the data. We thus conclude that while 50 fb^{-1} of data may suffice to enable one to distinguish the Higgs signal from continuum $\widetilde{Z}_2\widetilde{Z}_2$ production for smaller values of $\tan\beta$, integrated luminosities of 200–400 fb^{-1} may be necessary if $\tan\beta$ is large.

We should bear in mind that we have used only the shape of the 4ℓ mass distribution to try to untangle the Higgs bosons signal from continuum $\widetilde{Z}_2\widetilde{Z}_2$ production without any regard for rate or other event shape variables. It would be interesting to explore whether other distributions serve as better discriminators of the Higgs bosons from the continuum background.

V. CONCLUDING REMARKS

If low-energy supersymmetry is to provide a rationale for the stability of the electroweak scale, sparticles must all be lighter than about 1 TeV. In models where gaugino masses are unified at an ultrahigh unification scale, the lighter chargino and the two lightest neutralinos are frequently lighter than 100–150 GeV, and are thus expected to be kinematically accessible in the decays of the heavier Higgs bosons of the model. In a previous paper [7], we had shown within the MSSM framework that these SUSY modes dominated the decays of the heavier neutral Higgs boson, and particularly, the pseudoscalar Higgs boson over a wide range of SUSY parameters. This has two important consequences. The down side is that it reduces the cross sections for the $\gamma\gamma$ and ZZ or ZZ^* modes which form the usual signal for Higgs bosons at hadron colliders. These SUSY decays, however, open up new possibilities for Higgs boson detection, the most promising of which is the 4ℓ signal from the $\widetilde{Z}_2\widetilde{Z}_2$ decays of H_p or H_h. Here, we have improved on our previous computation of this signal, and also explored how it varies with model parameters. In this connection, we have used supergravity models as a guide in order to restrict the parameter space, and make this exploration tractable.

For the convenience of the reader, and also because the projected energy of the LHC has been reduced to 14 TeV, we first briefly review the detectability of the SM decay modes of the Higgs boson at the LHC. For the $\gamma\gamma$ signal, we require the center-of-mass scattering angle satisfy $\cos\theta^* < 0.8$ [29]. As before [3], the background is assumed to come from continuum pair production via $q\bar{q}, gg \to \gamma\gamma$ where the photons have $m_{\gamma\gamma} = m_H \pm 1\%$. For the ZZ and ZZ^* signal, we have required that the four leptons reconstruct to the Higgs boson mass within a mass-dependent resolution given in Ref. [7]. We have considered the $ZZ^* \to 4\ell$ signal only for $m_H > 130$ GeV, in which case backgrounds from continuum ZZ^* and $Z\gamma^*$ production have been shown to be negligible [30].

The regions of the $m_{H_p} - \tan\beta$ plane where these various signals are observable using the 99% C.L. criterion described in Ref. [3] is illustrated in Fig. 7 for (a) $m_{\tilde{g}} = m_{\tilde{q}} = -\mu = 1$ TeV, and (b) $m_{\tilde{g}} = m_{\tilde{q}} = -\mu = -300$

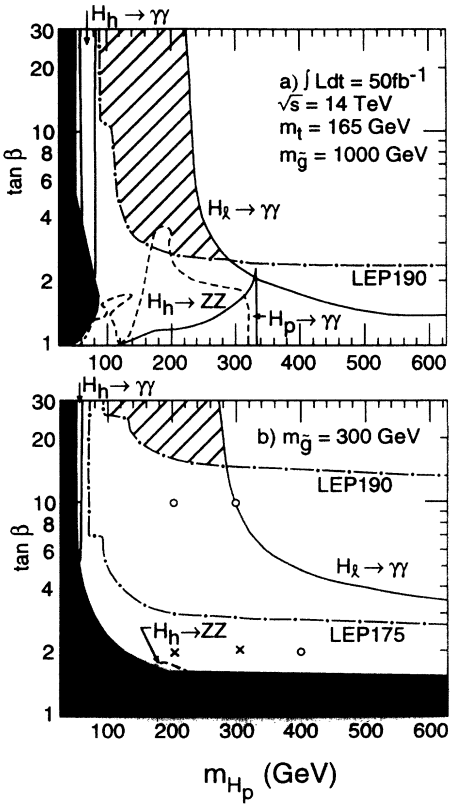

FIG. 7. Plot of discovery regions in the m_{H_p} vs $\tan\beta$ plane, at $\sqrt{s} = 14$ TeV, assuming an integrated luminosity of 50 fb^{-1}. In (a), we take $m_{\tilde{q}} = m_{\tilde{g}} = -\mu = 1000$ GeV, while in (b), we take $m_{\tilde{q}} = m_{\tilde{g}} = -\mu = 300$ GeV, so that SUSY decay of Higgs bosons are allowed. Other parameters are as in Fig. 1. The Higgs boson reach of LEP II is sensitive to the value of the A parameter. For large values of $|A|$, the LEP190 curve roughly follows the LEP175 curve as discussed in the text.

GeV. In this figure, we have assumed $A_t = A_b = 0$ and taken the integrated luminosity to be 50 fb^{-1}. The legends in this figure appear on the side of the boundary where the signal is observable. The black region denotes the range of parameters excluded by experiments at LEP [22] while the regions below the lines marked LEP190 and LEP175 can be probed in experiments at LEP with optimistic [$\sigma(H_\ell H_p)$ or $\sigma(H_\ell Z) > 0.05$ pb, $\sqrt{s} = 190$ GeV] and pessimistic [$\sigma(H_\ell H_p)$ or $\sigma(H_\ell Z) > 0.2$ pb, $\sqrt{s} = 175$ GeV] scenarios for performance of the LEP collider in its next phase. We note the following.

We have used an integrated luminosity of 50 fb^{-1} because at the reduced energy we found that the $H_\ell \to \gamma\gamma$ signal was essentially unobservable over the whole plane in Fig. 7(b) with a data sample of "just" 30 fb^{-1}. This is a reflection of the well-known fact that the position of this contour is extremely sensitive to the assumptions about the detector.

The shaded region is where none of the neutral Higgs bosons of the MSSM are detectable at either the LHC or at LEP II, at least via the signals discussed above. As noted in the Introduction, it may be possible to detect Higgs boson signals even for parameters inside this hole if the Higgs boson decays to τ leptons [6] or bottom quark pairs [11] are identifiable.

It is amusing to see that the shaded region actually shrinks in Fig. 7(b). This is somewhat misleading because this shrinkage is due to the upward movement of the LEP190 curve. Conservative assumptions about the performance of LEP considerably increase the region where there is no signal either at LEP II, or at the LHC. We have also checked that increasing the value of the A parameter lowers the LEP 190 curve. We have traced this to an increase in m_{H_ℓ}, and the corresponding suppression of the cross section for ZH_ℓ production: for $A_t = 400$ GeV or $A_t = -700$ GeV, the LEP 190 curve roughly follows the LEP175 curve in the figure. *Thus, the hole in Fig. 7(b) may well be considerably bigger than indicated by the shaded region even with optimistic assumptions about the performance of LEP II.*

We note here that the main reason for the change in the $H_\ell \to \gamma\gamma$ boundary when the parameters are altered from 1 TeV to 300 GeV is *not* the opening of the SUSY decays of H_ℓ. The shift occurs primarily because the Higgs boson mass is altered (due to the incorporation of the improved radiative corrections) resulting in a different size of the background.

Finally, we note that as anticipated, the region of parameters where the signal from two different Higgs bosons is simultaneously detectable is greatly reduced for the case in Fig. 7(b).

Turning to the neutralino signal for Higgs bosons, the cross sections for the 4ℓ signal from $\widetilde{Z}_2\widetilde{Z}_2$ decays of the Higgs bosons are summarized in Figs. 1–3. We see that these cross sections can be as large as 500 fb for ranges of model parameters allowed by all known experimental data. It is also worth noting that, before experimental cuts, the signal exceeds 10 fb over a large region of parameter space where there may be no visible SUSY signal even at LEP II. We have argued that there are no significant SM backgrounds to this signal. Thus while the detection of four lepton events at such rates will be a signal for new physics, its identification as a Higgs boson signal requires that it be separable from continuum $\widetilde{Z}_2\widetilde{Z}_2$ production for which the cross section is shown in Fig. 4, for $\mu = \pm m_{\tilde{g}}$ as expected in supergravity models. We see that over a large range of parameters this background is significantly smaller than the signal in Figs. 1–3. The efficiency with which this signal may be detected is shown in Table I, for cuts typical of LHC detectors. We see that this is typically 5–10 %, so that the cross sections in Figs. 1–3 correspond to 25–1000 events in an experimental data sample of 50 fb^{-1}.

In order to assess whether the Higgs signal could be distinguished above the neutralino continuum, we examined the mass distribution of the four leptons produced via the decay of the Higgs boson. For illustrative values of model parameters, we showed that the shape of this distribution may serve to discriminate the Higgs signal from continuum neutralino production provided $m_{H_p} \lesssim 2m_t$. We have argued that for low values of $\tan\beta$ an integrated luminosity of 50 fb^{-1} is sufficient for this discrimination, but an integrated luminosity of 200–400 fb^{-1} is required if $\tan\beta = 10$. We have, respectively, denoted these cases by crosses and open circles in Fig. 7(b). As we can see SUSY decays of Higgs bosons are indeed detectable well into the hole region if LEP II is operated at about 175 GeV. Although this is not obvious from the figure, this may also be the case with optimistic assumptions about the performance of LEP II, since, as we mentioned the LEP II observability curve essentially follows the LEP 175 curve if $|A_t|$ is large, while the Higgs signal, is relatively insensitive to variations in A_t.

In summary, we have shown that the processes $H_{h,p} \to \widetilde{Z}_2\widetilde{Z}_2 \to 4\ell + \not{E}_T$ lead to an observable rate for gold-plated four lepton events at the LHC for a significant range of SUSY model parameters. The parameter space region where the neutralino decays of SUSY Higgs bosons ought to be observable can be summarized as $2m_t > m_{H_p} > 2m_{\widetilde{Z}_2} \simeq 2m_{\tilde{g}}/3$, $m_{\tilde{q}} \sim m_{\tilde{g}}$ so that $m_{\tilde{\ell}} << m_{\tilde{q}}$ and $|\mu| \sim m_{\tilde{g}} \lesssim 500$ GeV, and $m_{H_p} \sim 200 - 350$ GeV. (We note that if SUSY parameters are in this region, there will also be a plethora of other signals via which SUSY will be detectable at the LHC [28].)

We have been unable to identify any significant SM background to this distinct SUSY Higgs boson signal. We have shown that this signal may be distinguished from continuum $\widetilde{Z}_2\widetilde{Z}_2$ production provided a sufficiently large integrated luminosity is available. Finally, this process may provide the only way to identify any Higgs boson of the MSSM if the model parameters are in the hole region (unless identification of their τ and bottom quark decays turns out to be feasible), and further, that it may well provide the only identifiable signal for the notoriously hard to detect pseudoscalar Higgs boson.

ACKNOWLEDGMENTS

This research was supported in part by the U.S. Department of Energy under Contracts No. DE-FG05-87ER40319 and No. DE-AM03-76SF00235. In addition, the work of H.B. was supported by the TNRLC.

[1] Y. Okada, M. Yamaguchi, and T. Yanagida, Phys. Lett. B **262**, 54 (1991); and Prog. Theor. Phys. **85**, 1 (1991); H. Haber and R. Hempfling, Phys. Rev. Lett. **66**, 1815 (1991); J. Ellis, G. Ridolfi, and F. Zwirner, Phys. Lett. B **257**, 83 (1991); R. Barbieri, M. Frigeni, and F. Caravaglios, *ibid.* **258**, 167 (1991); A. Yamada, *ibid.* **263**, 233 (1991).

[2] For a review of the MSSM, see H. P. Nilles, Phys. Rep. **110**, 1 (1984); P. Nath, R. Arnowitt, and A. Chamseddine, *Applied $N = 1$ Supergravity*, ICTP Series in Theoretical Physics, Vol. I (World Scientific, Singapore, 1984); H. Haber and G. Kane, Phys. Rep. **117**, 75 (1985); X. Tata, in *The Standard Model and Beyond*, edited by J. E. Kim (World Scientific, Singapore, 1991), p. 304; R. Arnowitt and P. Nath, Lectures presented at VII J. A. Swieca Summer School, Campos do Jordao, Brazil, 1993, Texas A & M Report No. CTP-TAMU-52/93, 1993 (unpublished).

[3] H. Baer, M. Bisset, C. Kao, and X. Tata, Phys. Rev. D **46**, 1067 (1992).

[4] J. Gunion and L. Orr, Phys. Rev. D **46**, 2052 (1992); for a review, see J. Gunion, in *Perspectives on Higgs Physics*, edited by G. Kane (World Scientific, Singapore, 1992).

[5] V. Barger, M. Berger, A. Stange, and R. Phillips, Phys. Rev. D **45**, 4128 (1992).

[6] Z. Kunszt and F. Zwirner, Nucl. Phys. **B385**, 3 (1992).

[7] H. Baer, M. Bisset, D. Dicus, C. Kao, and X. Tata, Phys. Rev. D **47**, 1062 (1993).

[8] H. Baer, D. Dicus, M. Drees, and X. Tata, Phys. Rev. D **36**, 1363 (1987); K. Griest and H. Haber, *ibid.* **37**, 719 (1988); J. Gunion, Phys. Rev. Lett. **72**, 199 (1994).

[9] G. Unal, D. Cavalli, L. Gozzi, and L. Perini, EAGLE Report No. PHYS-NO-005, 1992 (unpublished).

[10] It is possible that part, or even all, of the hole may eventually be closed by constraints from charged Higgs boson loop contributions to the process $b \to s\gamma$; within supersymmetry, this decay also receives contributions from other virtual sparticle loops which can cancel those from the charged Higgs bosons, especially from light charginos. For this reason, and because of some other theoretical uncertainties, we have not incorporated any constraints from this decay into our analysis. For an update, see F. Borzumati, Report No. DESY-93-090, 1993 (unpublished); M. Diaz, Phys. Lett. B **322**, 207 (1994).

[11] T. Garavaglia, W. Kwong, and D.-D. Wu, Phys. Rev. D **48**, 1899 (1993); J. Dai, J. Gunion, and R. Vega, Phys. Lett. B **315**, 355 (1993).

[12] A few of the many recent papers on this subject include J. Ellis and F. Zwirner, Nucl. Phys. **B338**, 317 (1990); G. Ross and R. G. Roberts, *ibid.* **B377**, 57 (1992); R. Arnowitt and P. Nath, Phys. Rev. Lett. **69**, 725 (1992); S. Kelly *et al.*, Nucl. Phys. **B398**, 3 (1993); M. Drees and M. Nojiri, *ibid.* **B369**, 54 (1992); G. Kane, C. Kolda, L. Roszkowski, and J. Wells, Report No. UM-TH-93-24, 1993 (unpublished); V. Barger, M. Berger, and P. Ohmann, Phys. Rev. D **49**, 4908 (1994).

[13] H. Baer and X. Tata, Phys. Rev. D **47**, 2739 (1993).

[14] The D-term corrections are proportional to $f_t^2 g^2$ or $f_b^2 g^2$, where the f_i denote the Yukawa couplings and g, the gauge couplings. Hence, their inclusion without the inclusion of pure gauge loops with contributions proportional to g^4 is formally consistent.

[15] See, e.g., V. Barger and R. J. N. Phillips, *Collider Physics* (Addison-Wesley, Redwood City, CA, 1990).

[16] D. A. Dicus and S. S. D. Willenbrock, Phys. Rev. D **39**, 751 (1989).

[17] E. Eichten, I. Hinchliffe, K. Lane, and C. Quigg, Rev. Mod. Phys. **56**, 759 (1984).

[18] A. B. Lahanas and D. V. Nanopoulos, Phys. Rep. **145**, 1 (1987).

[19] K. Inoue, A. Kakuto, H. Komatsu, and H. Takeshita, Prog. Theor. Phys. **68**, 927 (1982); **71**, 413 (1984).

[20] S. Martin and M. Vaughn, Phys. Lett. B **318**, 331 (1993).

[21] For QCD corrections to Higgs boson production, see S. Dawson, Nucl. Phys. **B359**, 283 (1991); A. Djouadi, M. Spira, and P. Zerwas, Phys. Lett. B **264**, 440 (1991); D. Graudenz, M. Spira, and P. M. Zerwas, Phys. Rev. Lett. **70**, 1372 (1993); R. P. Kauffman and W. Schaffer, Phys. Rev. D **49**, 551 (1994); M. Spira, A. Djouadi, D. Graudenz, and P. M. Zerwas, Phys. Lett. B **318**, 347 (1993). For QCD corrections to Higgs loop decays, see H.-Q. Zheng and D.-D. Wu, Phys. Rev. D **42**, 3760 (1990); S. Dawson and R. Kauffman, *ibid.* **47**, 1264 (1993); A. Djouadi, M. Spira, and P. Zerwas, Phys. Lett. B **311**, 255 (1993).

[22] Talk by G. Gopal at Aspen Winter Conference on "Particle Physics Before the Year 2000," Aspen, Colorado, January, 1994 (unpublished).

[23] See, e.g., Drees and Nojiri [12].

[24] V. Barger and T. Han, Phys. Lett. B **212**, 117 (1988).

[25] For $m_{\tilde{g}} = -\mu$, $\widetilde{Z}_{3,4}$ decay via two body modes so that their continuum production will not be confused with the signal. The same is frequently the case for other values of μ.

[26] F. Paige and S. Protopopescu, in *Supercollider Physics*, Proceedings of the Topical Conference Eugene, Oregon, 1985, edited by D. Soper (World Scientific, Singapore, 1986), p. 41; H. Baer, F. Paige, S. Protopopescu, and X. Tata, in *Proceedings of the Workshop on Physics at Current Accelerators and the Supercollider*, edited by J. Hewett, A. White, and D. Zeppenfeld (World Scientific, Singapore, 1993).

[27] V. Barger, A. Stange, and R. J. N. Phillips, Phys. Rev. D **44**, 1987 (1991).

[28] H. Baer, X. Tata, and J. Woodside, Phys. Rev. D **45**, 142 (1992).

[29] In our previous calculations, the $\gamma\gamma$ background had been underestimated since the photons were inadvertently required to satisfy $\cos\theta^* < 0.5$ instead of 0.8.

[30] The Solenoidal Detector Collaboration Technical Design Report No. SDC-92-201, 1992 (unpublished).

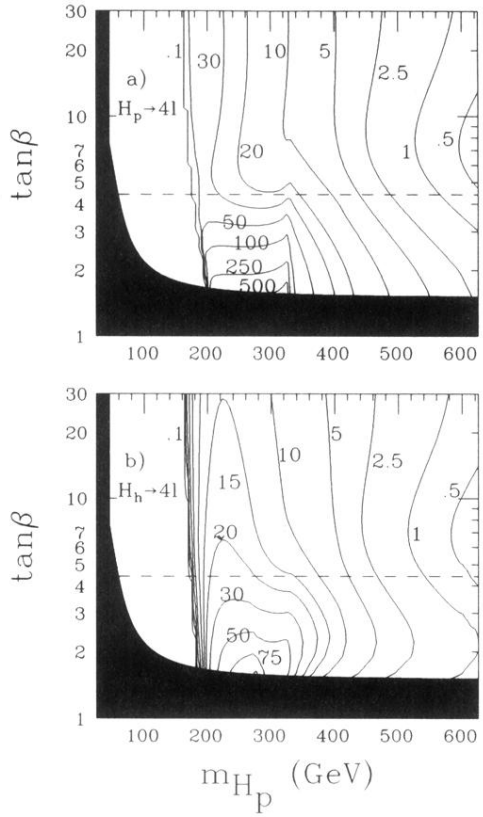

FIG. 1. Contour plot of cross section in fb for (a) $pp \to H_p \to \widetilde{Z}_2\widetilde{Z}_2 \to 4\ell + \not{E}_T$ and (b) $pp \to H_h \to \widetilde{Z}_2\widetilde{Z}_2 \to 4\ell + \not{E}_T$ events, in the m_{H_p} vs $\tan\beta$ plane, at $\sqrt{s} = 14$ TeV. We take $m_{\tilde{q}} = m_{\tilde{g}} = -\mu = 300$ GeV, $m_t = 165$ GeV, and $A_t = A_b = 0$. We also take $m^2_{\tilde{t}_L} = m^2_{\tilde{q}} - 50$ GeV^2 and $m^2_{\tilde{t}_R} = m^2_{\tilde{q}} - 100$ GeV^2. The region above the dashed lines corresponds to $m_{\widetilde{W}_1} < 90$ GeV, the approximate reach of LEP II. The reach of LEP II for detection of Higgs boson signals is shown in Fig. 7(b).

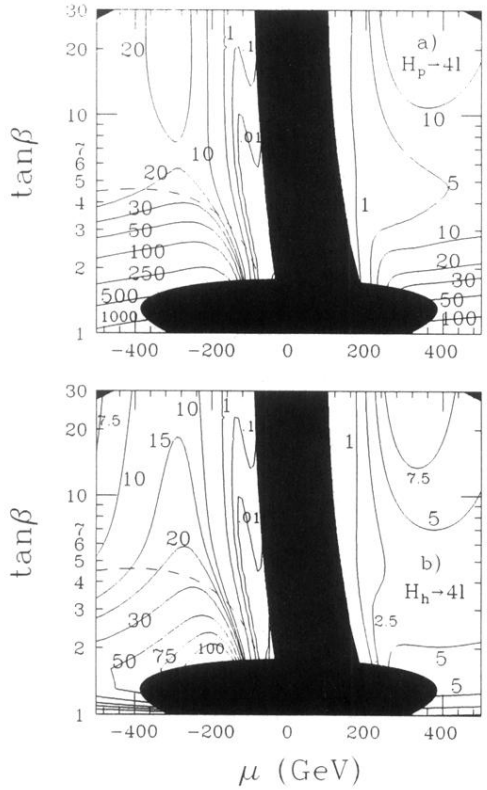

FIG. 2. Contour plot of cross section in fb for (a) $pp \to H_p \to \widetilde{Z}_2\widetilde{Z}_2 \to 4\ell + \not{E}_T$ and (b) $pp \to H_h \to \widetilde{Z}_2\widetilde{Z}_2 \to 4\ell + \not{E}_T$ events, in the μ vs $\tan\beta$ plane, at $\sqrt{s} = 14$ TeV. Parameters are as in Fig. 1, except $m_{H_p} = 250$ GeV. The region above the dashed contour corresponds to $m_{\widetilde{W}_1} < 90$ GeV.

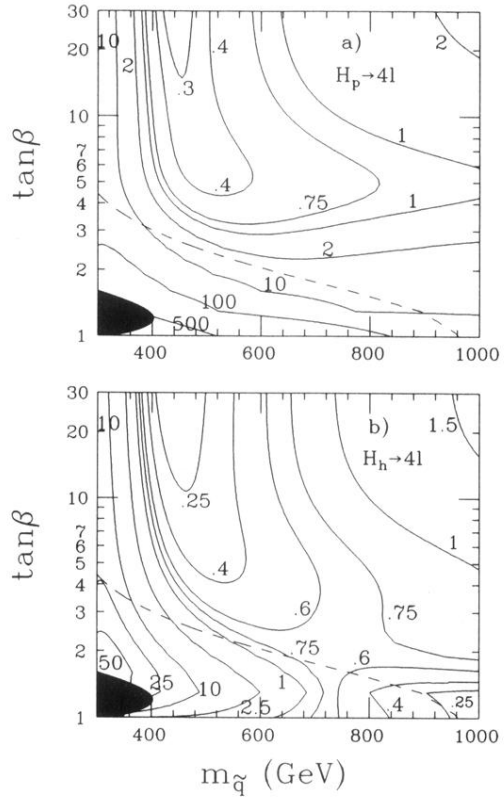

FIG. 3. Contour plot of cross section in fb for (a) $pp \to H_p \to \widetilde{Z}_2\widetilde{Z}_2 \to 4\ell + \not{E}_T$ and (b) $pp \to H_h \to \widetilde{Z}_2\widetilde{Z}_2 \to 4\ell + \not{E}_T$ events, in the $m_{\tilde{q}}$ vs $\tan\beta$ plane, at $\sqrt{s} = 14$ TeV. Parameters are as in Fig. 1, except $m_{H_p} = 250$ GeV. The region above the dashed contour corresponds to $m_{\widetilde{W}_1} < 90$ GeV.

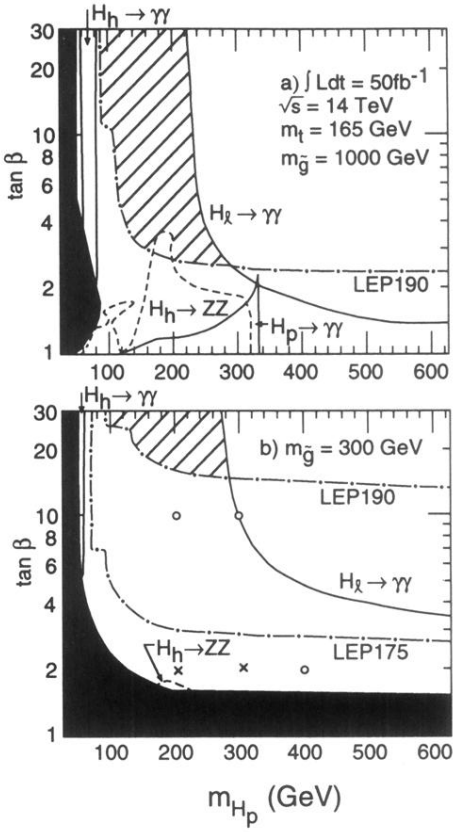

FIG. 7. Plot of discovery regions in the m_{H_p} vs $\tan\beta$ plane, at $\sqrt{s} = 14$ TeV, assuming an integrated luminosity of 50 fb^{-1}. In (a), we take $m_{\tilde{q}} = m_{\tilde{g}} = -\mu = 1000$ GeV, while in (b), we take $m_{\tilde{q}} = m_{\tilde{g}} = -\mu = 300$ GeV, so that SUSY decay of Higgs bosons are allowed. Other parameters are as in Fig. 1. The Higgs boson reach of LEP II is sensitive to the value of the A parameter. For large values of $|A|$, the LEP190 curve roughly follows the LEP175 curve as discussed in the text.